Geophysical Research Letters

RESEARCH LETTER
10.1029/2018GL077485

Key Points:
- The two large shocks of Amatrice and Norcia nucleated on distinct and parallel faults reactivated by high pore pressure in the footwall
- The irregular geometry of normal faults and reactivated ramps feeds in the complexity observed during coseismic ruptures and aftershocks
- Rapid definition of overpressurized volumes along the fault system has implications for the a priori identification of nucleation locations

Supporting Information:
- Figure S1
- Figure S2
- Supporting Information S1

Correspondence to:
C. Chiarabba,
claudio.chiarabba@ingv.it

Citation:
Chiarabba, C., De Gori, P., Cattaneo, M., Spallarossa, D., & Segou, M. (2018). Faults geometry and the role of fluids in the 2016–2017 Central Italy seismic sequence. *Geophysical Research Letters*, *45*, 6963–6971. https://doi.org/10.1029/2018GL077485

Received 6 FEB 2018
Accepted 9 JUL 2018
Accepted article online 13 JUL 2018
Published online 29 JUL 2018

Faults Geometry and the Role of Fluids in the 2016–2017 Central Italy Seismic Sequence

C. Chiarabba[1], P. De Gori[1], M. Cattaneo[1], D. Spallarossa[2], and M. Segou[3]

[1]Istituto Nazionale di Geofisica e Vulcanologia, Rome, Italy, [2]DIPTERIS, Università di Genova, Genoa, Italy, [3]British Geological Survey, Nottingham, UK

Abstract The 2016–2017 Central Italy seismic sequence ruptured overlapping normal faults of the Apennines mountain chain, in nine earthquakes with magnitude $Mw > 5$ within a few months. Here we investigate the structure of the fault system using an extensive aftershock data set, from joint permanent and temporary seismic networks, and 3-D *Vp* and *Vp*/*Vs* velocity models. We show that mainshocks nucleated on gently west dipping planes that we interpret as inverted steep ramps inherited from the late Pliocene compression. The two large shocks, the 24 August, $Mw = 6.0$ Amatrice and the 30 October, $Mw = 6.5$ Norcia occurred on distinct faults reactivated by high pore pressure at the footwall, as indicated by positive *Vp*/*Vs* anomalies. The lateral extent of the overpressurized volume includes the fault patch of the Norcia earthquake. The irregular geometry of normal faults together with the reactivated ramps leads to the kinematic complexity observed during the coseismic ruptures and the spatial distribution of aftershocks.

Plain Language Summary In this study we present refined earthquake locations and tomographic images of the upper crust to investigate the mechanisms of the 2016 Amatrice and Norcia destructive earthquakes. We find that earthquakes ruptured distinct segments of the fault system, partially reutilizing preexisting faults inherited from the previous compressional phase. Overpressurized fluids within the carbonate rocks facilitate the reactivation of faults during the large ruptures.

1. Introduction

In the Apennines, large earthquakes occur along the NW-SE trending normal faulting system, which accommodates about 2–3 mm/year of extension across the mountain range (Figure 1a). The recent Central Apennines sequence initiated in August 2016 covering within few months 60 km of the regional normal fault system (Barani et al., 2017; Chiaraluce et al., 2017; Tinti et al., 2016) between the 1997 Colfiorito and 2009 L'Aquila sequences (Chiarabba et al., 2009; Chiaraluce et al., 2004). Nevertheless, before the recent events seismicity was less pronounced in the epicentral area (Figure 1a).

During the sequence, this section of the fault system experienced a cascade of nine earthquakes larger than $Mw > 5.0$ on major and adjacent segments. The large events nucleated at the base of the southwest dipping normal fault system (Chiaraluce et al., 2017), with deeper hypocenters in the southern section (Figure 1b). The delayed activation of secondary faults with large magnitude aftershocks resulted in strong shacking on already damaged structures (Galli et al., 2017; QUEST Working Group, 2016; Tertulliani & e Azzaro, 2016).

The two largest mainshocks, the 24 August $Mw = 6.1$ Amatrice and the 30 October $Mw = 6.5$ Norcia, ruptured adjacent normal faults with ancillary structures (Cheloni et al., 2017, Livio et al., 2016) and with overlapping slip on shallow faults surfacing on the western slope of the Vettore mountain range (Galli et al., 2017; Pucci et al., 2017). While some authors have modeled the 24 August shock, as continuous slip on a single fault (Huang et al., 2017), others proposed bilateral rupture with hypocenter located in between two separate faults (Liu et al., 2017; Ren et al., 2017; Tinti et al., 2016). The relatively young normal faults accommodate the 2–3 mm/year of extension across the mountain range. The NNW trending extensional belt crosscuts large-scale thrust units developed during the Neogene compression and expressed by east verging thrusts with a progressive eastward migration (Bigi et al., 2011; Pierantoni et al., 2013; Scisciani et al., 2014; see Figure 1a). Such inherited structures are thought to play the role of lateral barriers during the coseismic propagation of earthquakes ruptures (Pizzi et al., 2017). Recent studies on the strongest earthquakes of the sequence (Calderoni et al., 2017) confirm that along-strike rupture directivity is a persistent feature of normal faulting earthquakes in the Apennines.

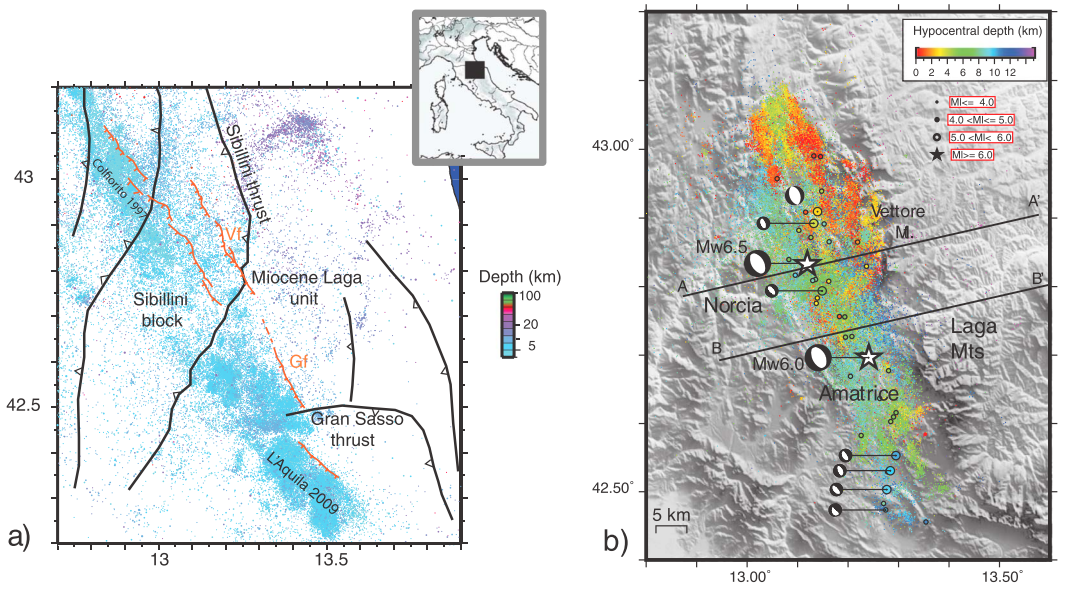

Figure 1. Map view of the seismicity in the central Apennines: (a) 1981–2016 (before 24 August), locations from the CSI catalog (Castello et al., 2006; Chiarabba et al., 2015). Main structural elements taken from Pierantoni et al. (2013) and Chiaraluce et al. (2005) are plotted (we only plot a subset of normal faults that is relevant for the paper discussion). The NW trending normal faulting system experienced multiple high-magnitude sequences over the past decades. Past decades seismicity is relatively poorer close to the 24 August and 30 October 2016 mainshocks (red stars); (b) 24 August 2016 to June 2017, as relocated in this work, focal mechanisms of the $Mw > 5.0$ earthquakes from Time Domain Moment Tensor solutions (see http://cnt.rm.ingv.it/tdmt). Hypocenters are shallower in northern portion of the fault system. Traces of cross sections in Figure 3 are shown.

Here we focus on the structure of the fault system and the role of fluids in the nucleation of mainshocks and evolution of the Amatrice sequence. We use about 50,000 aftershocks in order to image the *Vp* and *Vp/Vs* upper crustal structure by means of local earthquake tomography. We find multiple shallow splays rooting on gently west dipping faults that we interpret as preexisting ramps, inverted by high overpressure within the Sibillini thrust unit.

2. Data Analysis and Tomographic Inversion

In this study, we use earthquake arrival times recorded by 50 permanent and 20 temporary seismic stations deployed soon after the occurrence of the first, 24 August 2016 mainshock (Moretti et al., 2016). Three-component seismograms are automatically analyzed to determine the *P* and *S* wave phases for earthquake detection (Scafidi et al., 2016; Spallarossa et al., 2014). The automatic procedure resulted in about 100,000 earthquake detections for the time period from 24 August 2016 to June 2017 that were located using the most recent 1-D regional velocity model (Di Stefano et al. 2011). Especially for the 3-D inversion, we selected events with hypocentral solutions that have (1) a minimum number of 10 *P* and 5 *S* phases, (2) minimum distance of 10 km from the hypocenter to the closest station, (3) location errors less than 1 km, and (4) azimuthal gap less than $<180°$. In addition, we retained for each cell of a 2-km cube a maximum number of 10 events to optimize ray coverage within the investigated volume (see the supporting information). After that, a total of 44,177 earthquakes with 748,197 *P* wave and 656,484 *S-P* arrival times were inverted with the Simulps14 code (Haslinger, 1998). The iterative damped least squares algorithm solves for *Vp* and *Vp/Vs* in a 3-D grid with velocity values linearly interpolated through the medium and hypocentral/velocity parameters estimates progressively updated after parameter separation (Eberhart-Phillips & Michael, 1998; Um & Thurber, 1987). The tomographic model is discretized by a 3-D grid of nodes with $dx = dy = 5$ and $dz = 3$ km to optimize resolution and image fidelity. For each node, the initial *Vp* and *Vp/Vs* (= 1.85) were taken from the 1-D *Vp* model of Di Stefano et al. (2011) and the result of the Wadati regression, respectively. After five iteration steps, we obtained a final *rms* of 0.22 s corresponding to a variance improvement of 32%. See the supporting information for details on inversion statistics and errors.

To assess the reliability of the tomographic model, we analyzed, for each node, ray sampling and the full resolution matrix. We computed the Spread Function (SF) to quantify the compactness of each parameter averaging vectors and the Derivative Weight Sum to quantify the ray density around each node (Toomey & Foulger, 1989). We determined that a $SF = 3$ is the maximum limit below which the tomographic features could be considered reliable. The latter value is further confirmed by the analysis of the smearing directions by contouring, at each node, the volume where the resolution is 70% of the diagonal element (Reyners et al., 1999). We find that nodes having SF smaller than, or equal to, 3 have compact averaging vectors with negligible smearing effects.

3. Velocity Anomalies and Aftershocks Relocation

The *P* wave velocity (Figure 2) shows a main central NNW-SSE trending positive body that corresponds to the carbonate rocks that extensively outcrop in the area. The structural architecture of the Neogene compressional stage is largely evident in tomographic images (Figures 2 and 3). The high velocity Ceno-Mesozoic sedimentary rocks are deformed within the east verging thrust units that form the Sibillini and Laga mountain ranges (Pierantoni et al., 2013; Scisciani et al., 2014). To the east of the carbonate mountain range, a broad negative anomaly is found at shallow depth (Figure 2, layer at 3-km depth in green), associated with the presence of Pliocene synorogenic formations on top of the carbonates thrust units (see Bigi et al., 2011). The *Vp* anomalies mark a first-order discontinuity between the Sibillini and Laga thrust units, that is, the Sibillini ramp (Centamore & Rossi, 2009), with the uplifted sedimentary units developing along distinct thrust faults. The spatial extent of the very high *Vp*/*Vs* anomalies at 3- and 6-km depth (Figure 2) is controlled by the frontal and lateral ramps of the Sibillini unit. Southeast of the Sibillini thrust and close to the hypocenter of the Amatrice event, low *Vp*/*Vs* anomalies are present. *Vp*/*Vs* anomalies can be related to different factors including lithology or pore pressure (Dvorkin et al., 1999; Lin et al., 2015). According to the relation between *Vp*/*Vs* and porosity (Castagna et al., 1985), lateral anomalies in the shallowest region could be explained in terms of lithological contrast between the hanging wall and footwall of the thrust juxtaposing carbonate (*Vp*/*Vs* = 1.9) and turbidites (*Vp*/*Vs* = 1.6). However, since the thrust below 2-km depth crosscuts carbonate units (see Bigi et al., 2011, and Figure 3), we favor the interpretation of high pore pressure (high *Vp*/*Vs*), based on the attitude of cracks that remain open while internally pressurized (Nur, 1972).

Figure 3 shows that seismicity aligns on gently west dipping planes, rooted on an east dipping plane at about 6- to 9-km depth, whereas shallow seismicity (3–4 km) on the deep segment connects with the surface expression on the western slope of the Vettore Mountain.

In order to gain higher location accuracy for early aftershocks, we have relocated those events occurring in the periods 24 August to 30 September and 30 October to 31 December (after the first and second mainshocks, respectively), by using the 3-D model and allowing the model parameters to iterate further along with hypocenter relocation. The two relocated aftershocks data sets include 9,540 and 34,0279 *P* wave, and 83,304 and 305,778 *S-P* from 6,412 and 16,870 earthquakes, respectively, yielding a further 6% of variance improvement after four iterations. Figure 4 shows the final hypocentral distribution of early aftershocks along and across the fault system. The *Mw*6.0 and *Mw*6.5 mainshocks occurs on two fault segments separated by the Sibillini lateral ramp.

4. Discussion

The 2016 Central Apennines sequence involved several distinct SW dipping segments of the Apennines normal faulting system (Chiaraluce et al., 2017). In this study, we focus on the 24 August and 30 October main shocks that ruptured contiguous segments of the system, apparently with repeated slip on overlapping patches of the same fault or closely spaced and subparallel (Cheloni et al., 2017; Pucci et al., 2017; Pizzi et al., 2017; Tinti et al., 2016). The coseismic rupture of the August earthquake is highly heterogeneous consisting of two separate slip patches, whereas the 30 October event is characterized by additional slip on multiple fault structures (Cheloni et al., 2017; Scognamiglio et al., 2018) including an ancillary and low-angle faults. Field work immediately after both the August and October events reports surface slip on several fault splays outcropping along the western slope of the Vettore Mountain (EMERGEO Working Group, 2016; Pucci et al., 2017), consistent with activation of the Vettore fault at depth (Galli et al., 2017; Pizzi et al., 2017). The critical questions that remain are the role of preexisting structures in controlling fault kinematics, the

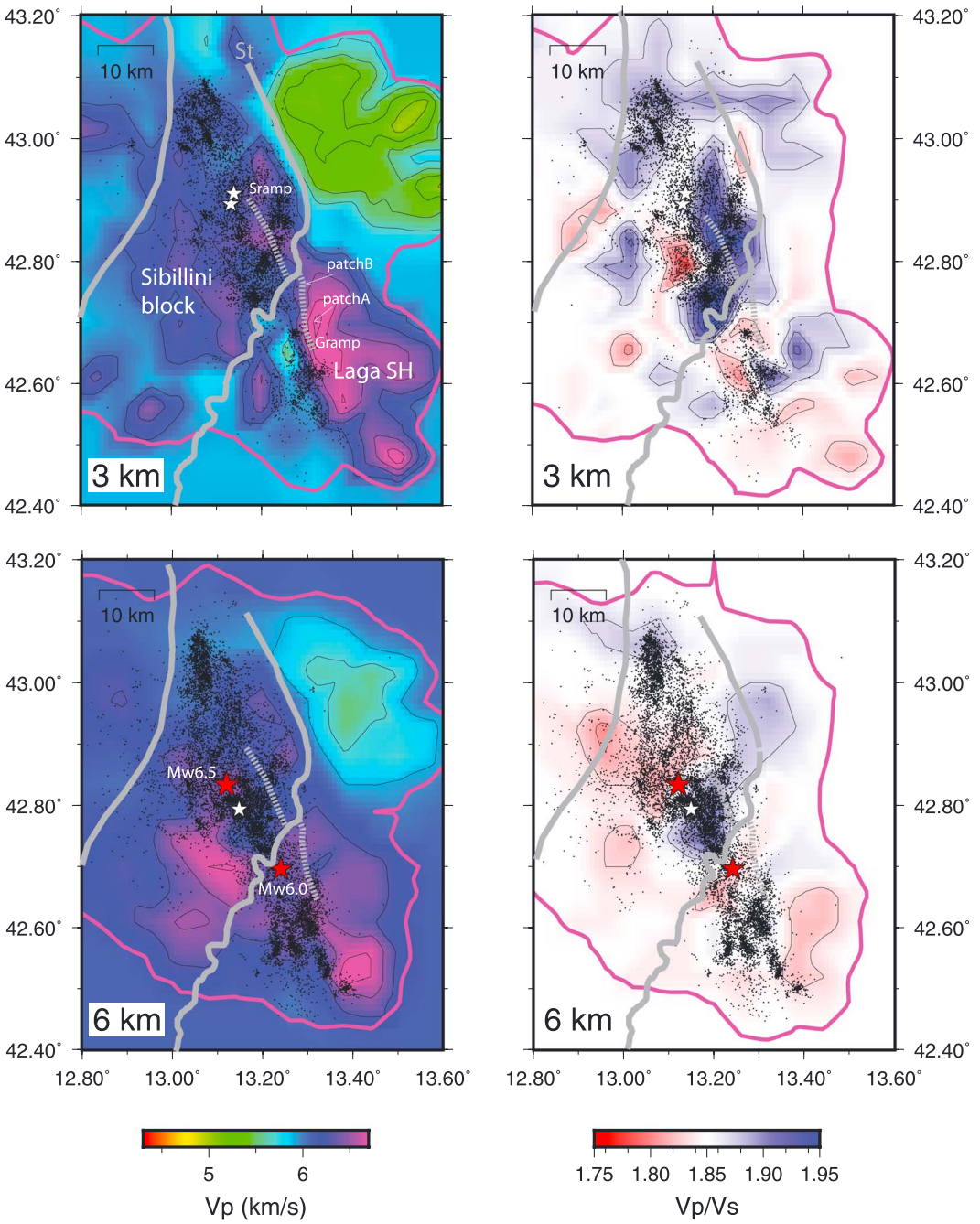

Figure 2. *Vp* and *Vp/Vs* layers at 3- and 6-km depth. Aftershocks (dots), large aftershocks and mainshocks (stars) occurring at ±1.5 km from each layer are shown. The gray lines are the main thrusts of the system, St = Sibillini thrust modified from Bigi et al. (2011). The dashed lines refer to the inferred tip of the blind ramps at depth (Gramp and Sramp for the 24 August and 30 October mainshocks, respectively). Magenta line is the limit of the well-resolved volume (*SF* = 3). Laga SH = Laga structural high.

condition of activation of closely spaced segments, and the connection between fault branching at shallow levels with the coseismic rupture. Interaction with preexisting compressional features is supported as a main factor controlling fault segmentation in the Apennines (Chiarabba & Amato, 2003; Chiaraluce et al., 2017), while other observations suggest that the high-angle normal fault planes crosscut the compressional features (Lavecchia et al., 2016; Porreca et al., 2018; Pucci et al., 2017). Our results help reveal the role of inherited structures and their contribution to the overall complexity of the two mainshock ruptures.

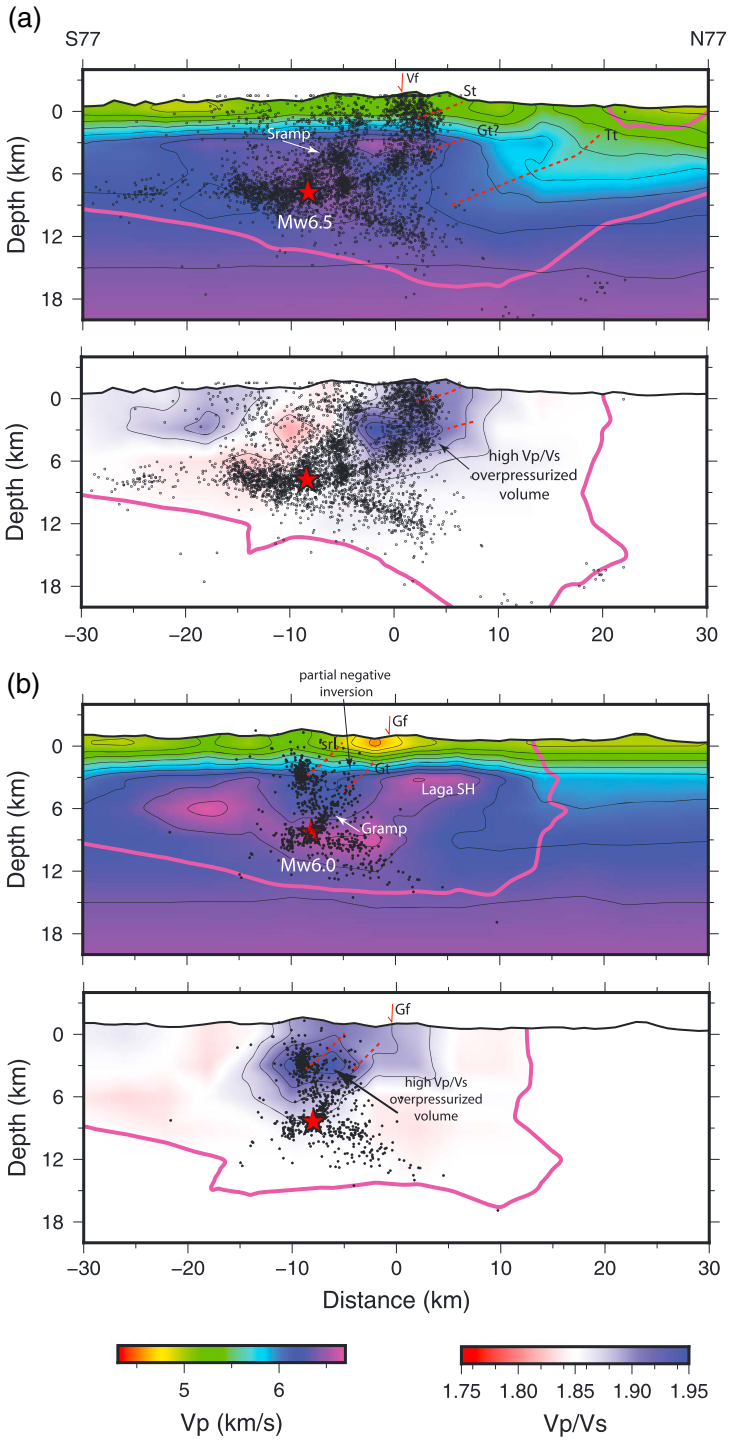

Figure 3. Vertical sections of *Vp* and *Vp/Vs* and relocated aftershocks across the fault system, close to the 30 October (a) and the 24 August 24 (b) mainshocks. Magenta line is limit of the well-resolved volume (Spread Function = 3). Seismicity describes two main west dipping planes that correspond to preexisting ramps of the compressional belt: The Gramp and the Sramp. In the section across the *Mw*6.0 event, only seismicity that occurred before the second mainshock is plotted. High *Vp/Vs* is present in the fault footwall, accounting for overpressurization consistent with persistent seismicity. Dashed red lines are the Sibillini (St) and Gran Sasso (Gt) thrusts defined in Centamore and Rossi (2009), whose geometry is drawn according to the positive warping in the *Vp* model. Note that the Gt at depth continues with the Gramp. The location of this structure at the border of the Laga SH supports the interpretation that this ramp was a Mesozoic normal fault inverted during the Pliocene compression. Vf and Gf are the Vettore and the Gorzano faults, according to Galadini and Galli (2003); LSH = Laga structural high.

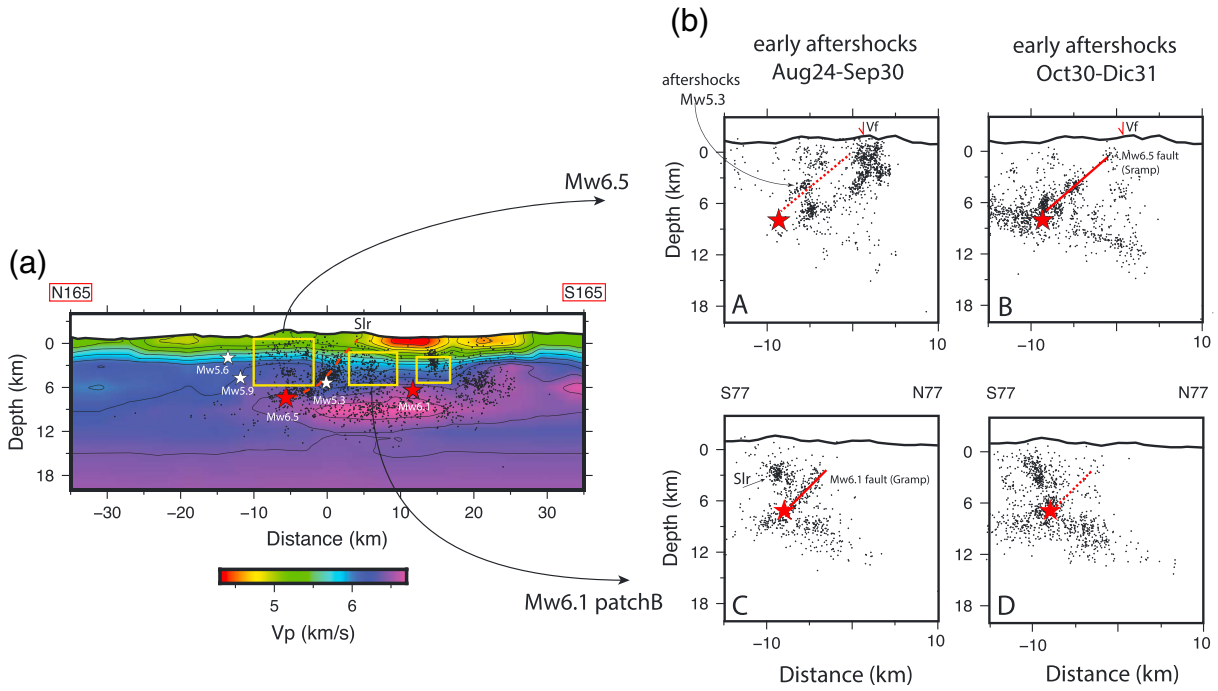

Figure 4. (a) Vertical section along the fault system and early aftershocks of the first mainshock. The boxes indicate the 30 October (to the left) and the 24 August patches (to the right), while mainshocks and *Mw*> 5.3 hypocenters are shown by stars. The red line indicates the lateral Sibillini ramp that segment the fault system. (b) The early aftershocks of the *Mw*6.0 and the *Mw*6.5 shocks are plotted, relatively to the two main patches located on either side of the Sibillini ramp. Cross sections are zoom on the faults, while the original traces are the same as sections plotted in Figure 3. Early aftershocks align on the two faults north and south of the Sibillini lateral ramp (slr; see sections B and C). Note the disappearance of aftershocks on the *Mw*6.0 fault and the onset of aftershocks on the *Mw*6.5 fault, after 30 October (section B).

Aftershock alignments in correspondence to warping of *Vp* and *Vp/Vs* anomalies suggest that the two ruptured faults correspond to preexisting ramps, inherited from the late Pliocene compression (Figures 2 and 3) now reactivated within the same sequence. The overall trend of these structures agrees with that constrained for the main faults by source modeling (Cheloni et al., 2017; Liu et al., 2017, Scognamiglio et al., 2018). The 24 August Amatrice mainshock ruptured two separate patches on a high-angle segment (Gramp) located at the border of a high *Vp* Mesozoic structural high (Laga SH in Figure 3b). The 30 October Norcia mainshock nucleated on a buried deep ramp (Sramp in Figure 3a) and propagated on shallow high-angle splays reaching the surface on the Vettore Mountain slope. The two faults are mechanically separated by the Sibillini lateral ramp (Figure 4). Early aftershocks of the two main shocks separate distinctly on the ramps, turning on and off after the two events (Figure 4b, sections A–D). Although we agree that preexisting compressional structure drives the segmentation of the normal fault system, our results clarify that the Sibillini lateral ramp (OAS in Chiaraluce et al., 2017) separates the fault segments ruptured during the two mainshocks and not the two patches ruptured during the first *Mw*6.0 shock. The shallow normal faults together with the reactivated ramps create an irregular geometry that leads to the complexity observed during the coseismic ruptures and the spatial distribution of aftershocks. Our results reconcile previous observations that normal faulting earthquakes in this sector of the Apennines reactivated thrust planes of the Pliocene compressional tectonics (Amato et al., 1998).

In the Apennines, the reactivation of preexisting faults and the occurrence of multiple mainshocks sequences are favored by high fluid pressure (Di Luccio et al., 2010; Malagnini et al., 2012), usually defined by high *Vp/Vs* anomalies in the upper crust (Chiarabba et al., 2009; Dvorkin et al., 1999). High *Vp/Vs* are observed within the Sibillini block (Figures 2 and 3), indicating high pore pressure within the upper portion of the fault system, confined by the Sibillini thrust. We identify this as the triggering mechanism of persistent aftershocks within the shallow section of the system. More strikingly, high *Vp/Vs* anomalies matches the length of the segment ruptured during the October mainshock and are observed close to the hypocenter (Figure 5), suggesting that fluids may have played a role in triggering the large rupture. The *Vp/Vs* distribution along the fault is

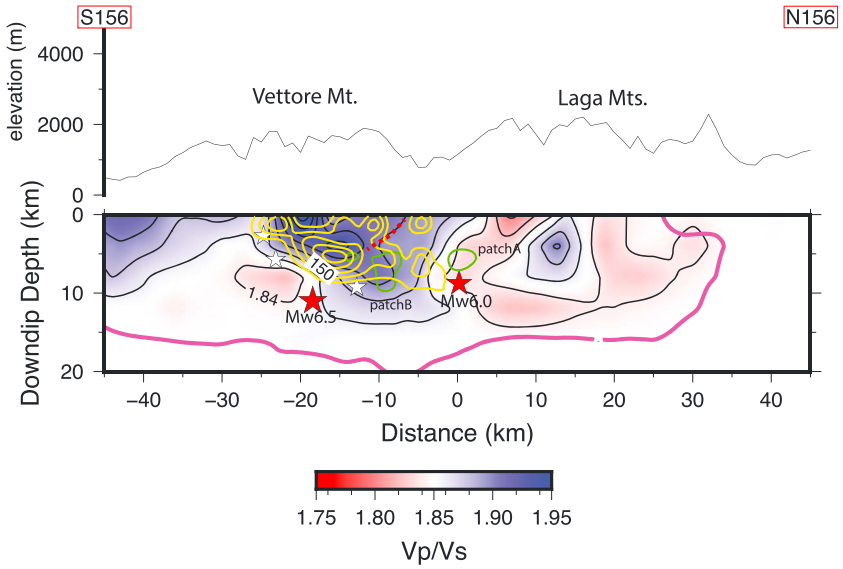

Figure 5. Downdip section of *Vp/Vs* on a 50° SSW dipping plane. The slip of the mainshocks is shown (from Scognamiglio et al., 2018), contour every 50 cm for the two mainshocks. The slip of the 24 August event, which occurred on a subparallel fault, is projected on the October fault plane. A common section for the two mainshocks is shown for simplicity. Note the high *Vp/Vs* on the fault patch with high coseismic slip during both the 24 August (patchB) and 30 October.

consistent with a process of fluid pressurization within the carbonate unit that persisted after the first event of August and culminated in the rupture of the main asperity during the October main shock.

A poorly developed cluster of aftershocks is consistent with the low *Vp/Vs* anomalies at the proximity of the Amatrice hypocenter in the southern edge of the activated system (Figures 2 and 5) suggesting a limited fluid pressurization.

5. Conclusions

Seismic tomography and aftershock distributions suggest that the two large ruptures of the 24 August, Amatrice, and the 30 October, Norcia, earthquakes nucleated on two faults, separated by the Sibillini lateral ramp, involving the reactivation of inherited inverted steep ramps formed during the late Pliocene compressive phase. We find that the high *Vp/Vs* anomalies in the shallow fault footwall support the idea that the evolution of the earthquake sequence was partly controlled by high pore pressure that favors the positive inversion of inherited structures and their subsequent reactivation.

Acknowledgments
We thank all the researchers and technicians involved during the seismic sequence taking care of safety in field surveys and management of instruments and data: Milena Moretti and the Sismiko group. Special thanks to Lauro Chiaraluce, Mauro Buttinelli, and Giuseppe Pezzo for helpful discussion. Comments by the Editor and two anonymous reviewers were very helpful and appreciated. Waveforms of aftershocks data can be retrieved in the EIDA database, https://www.orfeus-eu.org/data/eida/. Seismic data and models can be retrieved at ftp://ftp.ingv.it/pub/pasquale.degori/GL077485.

References

Amato, A., Azzara, R. M., Chiarabba, C., Cimini, G. B., Cocco, M., Di Bona, M., et al. (1998). The 1997 Umbria-Marche, Italy, earthquake sequence: A first look at the main shocks and aftershocks. *Geophysical Research Letters*, *25*(15), 2861–2864. https://doi.org/10.1029/98GL51842

Barani, S., Mascandola, C., Serpelloni, E., Ferretti, G., Massa, M., & Spallarossa, D. (2017). Time-space evolution of seismic strain release in the area shocked by the august 24-October 30 Central Italy seismic sequence. *Pure and Applied Geophysics*, *174*(5), 1875–1887. https://doi.org/10.1007/s00024-017-1547-5

Bigi, S., Casero, P., & Ciotoli, G. (2011). Seismic interpretation of the Laga basin: Constraints on the structural setting and kinematics of the Central Apennines. *Journal of the Geological Society*, *168*(1), 179–190. https://doi.org/10.1144/0016-76492010-084

Calderoni, G., Rovelli, A., & Giovambattista, R. (2017). Rupture directivity of the strongest 2016–2017 central Italy earthquakes. *Journal of Geophysical Research: Solid Earth*, *122*, 9118–9131. https://doi.org/10.1002/2017JB014118

Castagna, J. P., Batzle, M. L., & Eastwood, R. L. (1985). Relationship between compressional-wave and shear-wave velocities in clastic silicate rocks. *Geophysics*, *50*(4), 571–581. https://doi.org/10.1190/1.1441933

Castello, B., Selvaggi, G., Chiarabba, C., & Amato, A. (2006). *CSI Catalogo della sismicità italiana1981–2002*, versione 1.1. Roma: INGV-CNT.

Centamore, E., & Rossi, D. (2009). Neogene-Quaternary tectonics and sedimentation in the Central Apennines. *Bollettino Della Società Geologica Italiana*, *128*(1), 73–88.

Cheloni, D., de Novellis, V., Albano, M., Antonioli, A., Anzidei, M., Atzori, S., et al. (2017). Geodetic model of the 2016 Central Italy earthquake sequence inferred from 872 InSAR and GOS data. *Geophysical Research Letters*, *44*, 6778–6787. https://doi.org/10.1002/2017GL073580

Chiarabba, C., & Amato, A. (2003). *Vp* and *Vp/Vs* images in the Mw 6.0 Colfiorito fault region (central Italy): A contribution to the understanding of seismotectonic and seismogenic processes. *Journal of Geophysical Research*, *108*(B5), 2248. https://doi.org/10.1029/2001JB001665

Chiarabba, C., Amato, A., Anselmi, M., Baccheschi, P., Bianchi, I., Cattaneo, M., et al. (2009). The 2009 L'Aquila (Central Italy) MW6.3 earthquake: Main shock and aftershocks. *Geophysical Research Letters*, *36*, L18308. https://doi.org/10.1029/2009GL039627

Chiarabba, C., De Gori, P., & Mele, F. (2015). Recent seismicity of Italy: Active tectonics of the central Mediterranean region and seismicity rate changes after the Mw 6.3 L'Aquila earthquake. *Tectonophysics*, *638*, 82–93. https://doi.org/10.1016/j.tecto.2014.10.016

Chiaraluce, L., Amato, A., Cocco, M., Chiarabba, C., Selvaggi, G., Di Bona, M., et al. (2004). Complex normal faulting in the Apennines thrust-and-fold belt: The 1997 seismic sequence in central Italy. *Bulletin of the Seismological Society of America*, *94*(1), 99–116. https://doi.org/10.1785/0120020052

Chiaraluce, L., Barchi, M. A., Collettini, C., Mirabella, F., & Pucci, S. (2005). Connecting seismically active normal faults with Quaternary geological structures in a complex extensional environment: The Colfiorito 1997 case history (Northern Apennines, Italy). *Tectonics*, *24*, TC1002. https://doi.org/10.1029/2004TC001627

Chiaraluce, L., Di Stefano, R., Tinti, E., Scognamiglio, L., Michele, M., Casarotti, E., et al. (2017). The 2016 Central Italy seismic sequence: A first look at the mainshocks, aftershocks and source models. *Seismological Research Letters*, *88*(3), 757–771. https://doi.org/10.1785/0220160221

Di Luccio, F., Ventura, G., Di Giovambattista, R., Piscini, A., & Cinti, F. R. (2010). Normal faults and thrusts reactivated by deep fluids: The 6 April 2009 Mw 6.3 L'Aquila earthquake, central Italy. *Journal of Geophysical Research*, *115*, B06315. https://doi.org/10.1029/2009JB007190

Di Stefano, R., Chiarabba, C., Chiaraluce, L., Cocco, M., De Gori, P., Piccinini, D., & Valoroso, L. (2011). Fault zone properties affecting the rupture evolution of the 2009 (mw 6.1) L'Aquila earthquake (central Italy): Insights from seismic tomography. *Geophysical Research Letters*, *38*, L10310. https://doi.org/10.1029/2011GL047365

Dvorkin, J., Mavko, G., & Nur, A. (1999). Overpressure detection from compressional- and shearwave data. *Geophysical Research Letters*, *26*(22), 3417–3420. https://doi.org/10.1029/1999GL008382

Eberhart-Phillips, D., & Michael, A. J. (1998). Seismotectonics of the Loma Prieta, California, region determined from three-dimensional *VpVp/Vs*, and seismicity. *Journal of Geophysical Research*, *103*, 21,009–21,120.

EMERGEO Working Group (2016). Coseismic effects of the 2016 Amatrice seismic sequence: First geological results. *Annales de Geophysique*, *59*(5). https://doi.org/10.4401/ag-7195

Galadini, F., & Galli, P. (2003). Paleoseismology of silent faults in the Central Apennines (Italy): The Mt. Vettore and Laga Mts. Faults. Annals of. *Geophysics*, *46*(5), 815–836.

Galli, P., Castenetto, S., & Peronace, E. (2017). The macroseismic intensity distribution of the October 30, 2016 earthquake in central Italy (Mw 6.6). Seismotectonic implications: 2016 central Italy earthquake intensity. *Tectonics*, *36*, 2179–2191. https://doi.org/10.1002/2017TC004583

Haslinger, F. (1998). Velocity structure, seismicity and seismotectonics of northwestern Greece between the Gulf of Arta and Zakynthos, PhD thesis, Dep. Geophys., ETH, Zurich, Switzerland.

Huang, M.-H., Fielding, E. J., Liang, C., Milillo, P., Bekaert, D., Dreger, D., & Salzer, J. (2017). Coseismic deformation and triggered landslides of the 2016 Mw 6.2 Amatrice earthquake in Italy. *Geophysical Research Letters*, *44*, 1266–1274. https://doi.org/10.1002/2016GL071687

Lavecchia, G., Castaldo, R., de Nardis, R., De Novellis, V., Ferrarini, F., Pepe, S., et al. (2016). Ground deformation and source geometry of the 24 August 2016 Amatrice earthquake (Central Italy) investigated through analytical and numerical modeling of DInSAR measurements and structural-geological data. *Geophysical Research Letters*, *43*, 12,389–12,398. https://doi.org/10.1002/2016GL071723

Lin, J. Y., Hsu, S.-K., Lin, A., Yeh, Y.-C., & Lo, C.-L. (2015). *Vp/Vs* distribution in the northern Taiwan area: Implications for the tectonic structures and rock property variations. *Tectonophysics*, *692*, 181–190. https://doi.org/10.1016/j.tecto.2015.09.013

Liu, C., Zheng, Y., Xie, Z., & Xiong, X. (2017). Rupture features of the 2016 Mw 6.2 Norcia earthquake and its possible relationship with strong seismic hazards. *Geophysical Research Letters*, *44*, 1320–1328. https://doi.org/10.1002/2016GL071958

Livio, F., Michetti, A. M., Vittori, E., Gregory, L., Wedmore, L., Piccardi, L., et al. (2016). Surface faulting during the August 24, 2016, Central Italy earthquake (Mw 6.0): Preliminary results. *Annales de Geophysique*, *59*(5), 1–8. https://doi.org/10.4401/ag-7197

Malagnini, L., Lucente, F. P., De Gori, P., Akinci, A., & Munafo, I. (2012). Control of pore fluid pressure diffusion on fault failure mode: Insights from the 2009 L'Aquila seismic sequence. *Journal of Geophysical Research*, *117*, B05302. https://doi.org/10.1029/2011JB008911

Moretti, M., Baptie, B., & Segou, M. (2016). SISMIKO: Emergency network deployment and data sharing for the 2016 central Italy seismic sequence. *Annales de Geophysique*, *59*(5). https://doi.org/10.4401/ag-7212

Nur, A. (1972). Dilatancy, pore fluids, and premonitory variations of Ts/Tp travel times. *Bulletin of the Seismological Society of America*, *62*, 1217–1222.

Pierantoni, P., Deiana, G., & Galdenzi, S. (2013). Stratigraphic and structural features of the Sibillini Mountains (Umbria-Marche Apennines, Italy). *Italian Journal of Geosciences (Boll. Soc. Geol. It.)*, *132*(3), 497–520. https://doi.org/10.3301/IJG.2013.08

Pizzi, A., Di Domenica, A., Gallovič, F., Luzi, L., & Puglia, R. (2017). Fault segmentation as constraint to the occurrence of the main shocks of the 2016 Central Italy seismic sequence. *Tectonics*, *36*, 2370–2387. https://doi.org/10.1002/2017TC004652

Porreca, M., Minelli, G., Ercoli, M., Brobia, A., Mancinelli, P., Cruciani, F., et al. (2018). Seismic reflection profiles and subsurface geology of the area interested by the 2016–2017 earthquake sequence (Central Italy). *Tectonics*, *37*, 1116–1137. https://doi.org/10.1002/2017TC004915

Pucci, S., de Martini, P. M., Civico, R., Villani, F., Nappi, R., Ricci, T., et al. (2017). Coseismic ruptures of the 24 august 2016, mw 6.0 Amatrice earthquake (central Italy). *Geophysical Research Letters*, *44*, 2138–2147. https://doi.org/10.1002/2016GL071859

QUEST working Group (2016). The 24 August 2016 Amatrice earth- quake: Macroseismic survey in the damage area and EMS intensity assessment. *Annals Geophysics*, *59*. https://doi.org/10.4401/ag-7203

Ren, Y., Wang, H., & Wen, R. (2017). Imprint of rupture directivity from ground motions of the 24 August 2016 Mw6.2 Central Italy earthquake. *Tectonics*, *36*, 3178–3191. https://doi.org/10.1002/2017TC004673

Reyners, M., Eberhart-Phillips, D., & Stuart, G. (1999). A three-dimensional image of shallow subduction: Crustal structure of the Raukumara Peninsula, New Zealand. *Geophysical Journal International*, *137*(3), 873–890. https://doi.org/10.1046/j.1365-246x.1999.00842

Scafidi, D., Spallarossa, D., Turino, C., Ferretti, G., & Viganò, A. (2016). Automatic *P-* and *ss*-wave local earthquake tomography: Testing performance of the automatic phase-picker engine "RSNI-picker". *Bulletin of the Seismological Society of America*, *106*(2), 526–536. https://doi.org/10.1785/0120150084

Scisciani, V., Agostini, S., Calamita, F., Pace, P., Cilli, A., Giori, I., & Paltrinieri, W. (2014). Positive inversion tectonics in foreland fold-and-thrust belts: A reappraisal of the Umbria–Marche Northern Apennines (Central Italy) by integrating geological and geophysical data. *Tectonophysics*, *637*, 218–237. https://doi.org/10.1016/j.tecto.2014.10.010

Scognamiglio, L., Tinti, E., Casarotti, E., Pucci, S., Villani, F., Cocco, M., et al. (2018). Complex fault geometry and rupture dynamics of the MW 6.5, 30 October 2016, Central Italy earthquake. *Journal of Geophysical Research: Solid Earth*, *123*, 2943–2964. https://doi.org/10.1002/2018JB015603

Spallarossa, D., Ferretti, G., Scafidi, D., Turino, C., & Pasta, M. (2014). Performance of the RSNI-Picker. *Seismological Research Letters*, *85*(6), 1243–1254. https://doi.org/10.1785/0220130136

Tertulliani A. e Azzaro R. [a cura di] (2016). *QUEST—Rilievo macrosismico per i terremoti nell'Italia centrale*. Aggiornamento dopo le scosse del 26 e 30 ottobre 2016, rapporto interno INGV, Roma. https://doi.org/10.5281/zenodo.182694

Tinti, E., Scognamiglio, L., Michelini, A., & Cocco, M. (2016). Slip heterogeneity and directivity of the ML 6.0, 2016, Amatrice earthquake estimated with rapid finite-fault inversion. *Geophysical Research Letters*, *43*, 10,745–10,752. https://doi.org/10.1002/2016GL071263

Toomey, D. R., & Foulger, G. R. (1989). Tomographic inversion of local earthquake data from the Hengill-Grensdalur central volcano complex, Iceland. *Journal of Geophysical Research*, *94*(B12), 17,497–17,510. https://doi.org/10.1029/JB094iB12p17497

Um, J., & Thurber, C. H. (1987). A fast algorithm for two-point seismic ray tracing. *Bulletin of the Seismological Society of America*, *77*, 972–986.